# Improved Analysis of Extreme Wind Loads on Low-Rise Structures

by

M. R. Hajj[1], D. A. Jordan[2], and H. W. Tieleman[1]

ABSTRACT

Characterizing atmospheric turbulence and determining the far-field velocity-pressure relation are important for simulation and prediction of extreme wind loads on structures. In this work, we show some shortcomings of Fourier decomposition and present wavelet analysis as a better suited technique for characterizing turbulence and modeling velocity-pressure relation. Examples from full and model scale experiments are presented. The results show that, with wavelet analysis, one could establish an intermittency character for atmospheric turbulence and relate low-pressure peaks to highly turbulent events in the atmospheric wind.

KEYWORDS: wind engineering, low-rise structures, turbulence, sepctral analysis, wavelet analysis.

## 1. INTRODUCTION

Over the past thirty years, there has been extensive research studies to mitigate against wind damage on structures. The results of many of these studies have found their way into building codes and have played an important role in reducing the extent of damage. Yet, it is fair to state that more improvements are needed in order to reduce losses. A simple comparison of wind tunnel experiments, code requirements, and full-scale measurements of pressure coefficients show a large scatter of data even for the simplest cases. These discrepancies are mainly due to the lack of consensus which has been hard to obtain because of the many variables and methods of analysis involved in determining wind loads. In particular, the atmospheric boundary layer is turbulent and consequently simulating turbulence characteristics is as important as simulating the mean flow. Moreover, the velocity-pressure relation is governed by Poissons equation which predicts that surface pressure is a function of the entire velocity field. Such equation has linear and nonlinear terms whereby the mean shear and turbulence contribute to the pressure. Consequently, two important questions would be: Is it possible to establish a model that predicts pressure from mean and turbulence parameters of the atmospheric wind? If so, which turbulence parameters should be considered? In this work, we present wavelet analysis as a suitable technique that could provide answers to these questions.

To date, Fourier decomposition has been the main tool used in the analysis and modeling of atmospheric turbulence and the velocity-pressure relation. The underlying process in Fourier decomposition is the representation of a time series, such as wind velocity or surface pressure, by a set of complex sinusoids. There are several advantages for such a representation. First, turbulence scales in the atmosphere can be represented by frequency components and their energy is obtained from the power spectrum. Second, estimates of spectral energy in particular frequency bands are statistically independent of the energy estimates in other bands. Third, for large sets of data, frequency decomposition can be obtained rapidly with FFT techniques. Fourth, higher-order moments can be used to determine nonlinear couplings among spectral components in one signal or between two signals, such as velocity and pressure. Finally, the velocity-pressure relation can be modeled by an input-output system that accounts for contributions from linear and nonlinear sources in the velocity fluctuations to the pressure.

The above mentioned advantages made the use of frequency domain analysis for the simulation and modeling of atmospheric turbulence and wind loads on structures very attractive. Yet, this analysis domain has many shortcomings which makes it of limited importance in characterizing wind flows for the purpose of predicting or simulating extreme wind loads on structures. The objectives of this paper are three-fold. The first is to discuss some shortcomings of frequency domain analysis when used to characterize the wind events that are of important value in prediction and simulation of wind loads on structures. The second is to present wavelet, i.e. time-scale, domain analysis as an alternative to the traditional frequency decomposition. In particular, we will show how quantita-

[1] Department of Engineering Science and Mechanics, Virginia Tech, Blacksburg, VA, 24061

[2] School of Engineering and Applied Science, University of Virginia, Charlottesville, VA 22903

tive information regarding extreme wind loads from the wavelet analysis can be derived. The third is to show how such information can be used to experimentally and numerically simulate or predict wind loads on structures. Examples from full and model scale experiments are presented.

## 2. SHORTCOMINGS OF FREQUENCY DOMAIN MODELS OF ATMOSPHERIC TURBULENCE

Models of normalized spectra of the velocity components of atmospheric wind have been developed to characterize energy content of turbulence scales which are represented by frequency components. The majority of these models are interpolation expressions between low-frequency and high-frequency asymptotes. Figures 1-a and 1-b show the time series of fifteen minutes records of the $u$- and $v$-velocity components obtained from the Wind Engineering Research Field Laboratory (WERFL) at Texas Tech. The sampling rate for these records is 10 Hz and the measurements were taken at an elevation, $H$, of about 4.0 m. The corresponding time record of the pressure coefficients at $x/H = 0.6$ and $y/H = 0.403$ is shown in figure 1-c. More information about the terrain and experimental set-up is given in Levitan and Mehta (1991). Those records were classified stationary by Smith and Mehta. A comparison of the power spectral density functions of these records and their respective analytical models (Tieleman (1994)) is given in figures 2-a and 2-b. The results clearly show that the observed spectra do not match the analytical models. This mismatch is due to the fact that, in our estimates of the spectra, no segment averaging was performed. Because only one segment was used, the variances of the spectra are equal to the estimated values. It should be noted here that when segment averaging was performed over a period of two hours, the estimated spectra became smooth and approached the analytical models. Yet, such an averaged spectra cannot be of any significant use in simulating or modeling low pressure peaks that take place over time periods of one to three seconds (see figure 1-c). These peaks cannot be related to average spectra estimated over a two-hour period. These peaks can only be related to time variations of the energy of turbulent fluctuations.

## 3. SHORTCOMINGS OF FREQUENCY-DOMAIN MODELING OF THE VELOCITY-PRESSURE RELATION

Several frequency-domain models have been proposed to establish a relation between incident velocity fluctuations and surface pressure fluctuations. These models are based on strip or quasi-steady approaches. In strip theory, the wind pressure is directly-related to the wind velocity at the same elevation Kawai (1983). In the linearized quasi-steady theory, the surface pressure fluctuations are considered to be directly proportional to instantaneous velocity and flow direction Kawai (1983). The modified (nonlinear version of) quasi-steady theory assumes that the flow is directly proportional to the squares of the fluctuating velocity components. Studies conducted to examine these theories show that, in general, they fail to predict many of the characteristics of the surface pressure fluctuations. This is especially true in the important regions of separation, vortex shedding and/or vortex formation. These results have lead to the idea of introducing frequency-dependent empirical aerodynamic admittance functions. Yet, measurements of these functions show large discrepancies. Often, it is assumed that these discrepancies arise from nonlinear effects that were not taken into consideration. In order to determine these effects, we performed analysis of nonlinear relations between velocity and pressure spectral components using higher-order statistical moments (Hajj et al. (1997)).

The extent to which spectral components in two signals are linearly correlated can be obtained from measurements of the linear coherence. For zero-mean stationary fluctuations $u(t)$ and $p(t)$, that represent random velocity and pressure waveforms, the linear coherence function, $\gamma^2_{up}$, is defined as

$$\gamma^2_{up} = \frac{|< P(f)U^*(f) >|^2}{\{< |U(f)|^2 >< |P(f)|^2 >\}} \qquad (1)$$

where $< ... >$ denotes time averaging and $U(f)$ and $P(f)$ are the complex Fourier amplitudes of $u(t)$ and $p(t)$ respectively. As explained by Hajj et al. (1997), the next higher-order spectral moments to the cross-power spectrum, namely the cross-bispectrum, can be used to investigate the nonlinear coupling among spectral components, with different frequencies, in two signals. For the velocity and pressure waveforms, the cross-bispectrum is defined as

$$S_{uup}(f_i, f_j) =< P(f_k)U^*(f_i)U^*(f_j) > \qquad (2)$$

where $f_k$ is the algebraic sum of $f_i$ and $f_j$. As defined here, the cross-bispectrum is a function of two frequency components and measures the degree of coherence among modes with frequencies $f_k$ in the pressure spectrum and $f_i$ and $f_j$ in the velocity spectrum. If the

three modes are independent, their phases are statistically independent and subsequently, the phase of the cross-bispectrum is randomly distributed. The averaging, indicated in equation (2) by $< ... >$, yields a zero value for the cross-bispectrum. On the other hand, if the three modes are nonlinearly related, a phase coherence will exist among them and the averaging will result in a nonzero value for the cross-bispectrum. The normalized value of the cross-bispectrum is termed the cross-bicoherence and is given by

$$b^2_{uup}(f_i, f_j) = \frac{|S_{uup}(f_i, f_j)^2}{< |U(f_i)U(f_j)|^2 >< |P(f_k)|^2 >} \quad (3)$$

and, by Schwartz inequality, varies between zero and one.

In order to assess the extent of the nonlinear relation between spectral components of the velocity and pressure fluctuations, simultaneously measured velocity and pressure fluctuations were obtained from the Clemson wind-tunnel. The experimental model is a 1/50 scale of the experimental building at WERFL. Details of the experimental setup are given in Hajj et al. (1996). The wind tunnel data was chosen because higher-order statistical analysis require long data records that are stationary. Such data could not be obtained from full scale measurements. Spectra of the $u$-velocity component of the incident flow and of the pressure fluctuations at the corresponding point on the roof surface and the linear coherence between the two signals are shown in figures 3 and 4, respectively. The resulting pressure spectra show two broadband peaks around $fH/U = 0.02$ and 0.5. The linear coherence measurements reveal that only the very low-frequency band ($fH/U < 0.01$) in the velocity and pressure are linearly correlated. Beyond this band there is no indication of any linear coherence. By comparison of figures 3 and 4, the range of frequencies where relatively high velocity-pressure coherence occurs contains only a small portion of the spectral energy. Figure 5 shows contour plots of the cross-bicoherence between the velocity and pressure fluctuations. The results show that a low level of bicoherence is measured among all pairs of frequency components for the velocity and the pressure fluctuations. Such a low level (<0.1) shows that there is no direct nonlinear coupling between the frequency components in the pressure and the far-field velocity fluctuations.

The above results show that, while low-frequency components ($fH/U < 0.01$) in the incident turbulence and pressure fluctuations are linearly coupled, the relatively higher frequency components, which contain energy, are not coupled. These results are true for different angles of incidence and different flow configurations. Measurements of the cross-bicoherence show that the nonlinear effects are not the major cause for the low linear coherence in the high frequency range. These results show that the relation between frequency components of the incident velocity and pressure fluctuations is not direct and cannot be quantified. This is mainly due to segment averaging and elmination of temporal information.

## 4. DEFINITIONS AND IMPLEMENTATION PROCEDURES AND WAVELET DOMAIN ANALYSIS

As discussed in the previous section, one major shortcoming of frequency domain analysis is that it does not provide temporal information. Such information can be obtained from short-time Fourier transform or the Gabor transform. However, it is proposed to use wavelets for two reasons. First, the wavelet analysis has the advantage of providing a better time-scale resolution. A short-time Fourier transform uses a single analysis window. Consequently, the time-frequency resolution is fixed over the entire time-frequency plane. In contrast, the wavelet transform uses short windows at high frequencies and long windows at low frequencies. Because wind velocity components can contain low-frequency components over long durations and relatively high-frequency components of short duration, wavelet analysis is a more suitable technique than Fourier analysis. Second, while frequency analysis is performed by projecting a signal onto a number of sinsoids which are infinite in extent, wavelet analysis is performed by projecting the signal onto a set of highly localized basis functions. These basis functions are called wavelets and are obtained from a single "mother" wavelet by dilations and translations. Thus, in wavelet analysis, the notion of a scale replaces that of frequency which leads to the so-called time-scale representation. Because it is localized in time, a scale representation is more suitable than a frequency representation for examining temporal characteristics of turbulence.

Given a time signal, $f(t)$, its continuous wavelet transform is defined as

$$\mathcal{W}(a, \tau) =< f(t), \psi_{a,\tau} >= \int_{-\infty}^{\infty} f(t)\psi^*_{a,\tau}(t)dt, \quad (4)$$

with

$$\psi_{a,\tau} = a^{-\frac{1}{2}}\psi\left(\frac{t-\tau}{a}\right), \quad (5)$$

where $\psi_{a,\tau}$ is a function called a wavelet, $a$ is a dilation parameter, $\tau$ is a translation or shift parameter and the $*$ denotes complex conjugate, when the wavelet is complex. The wavelet transform coefficients, $\mathcal{W}(a,\tau)$, represent the contribution of scales $a$ to the signal at time, $\tau$. Wavelet energy is defined from the wavelet coefficients as $\mathcal{W}\mathcal{W}^*$. From Farge (1992), a wavelet energy density (energy per scale size) can be defined as $\mathcal{W}\mathcal{W}^*/a$. When integrated over time, the wavelet energy density yields the global wavelet energy spectrum which gives the energy content at that scale.

In the following, we use a complex Morlet mother function which is given by

$$\psi(t) = exp(i\omega_\psi t)exp(-|t|^2/2), \qquad (6)$$

where $\omega_\psi$ is a constant that forces the wavelet to be admissible, i.e., it possess an inverse transform, the complex Morlet wavelet has been shown to have several advantages over real wavelet functions. The digital implementation of the continuous wavelet transform is a discrete convolution between the sampled time series and sampled versions of the analyzing wavelet at all scales. All scaled versions of the complex Morlet wavelet were sampled with enough samples to avoid aliasing and the convolutions were performed in the frequency domain using the FFT. A relationship can be established between the wavelet scale and the peak frequency, $f_p$, of the scaled wavelet bandpass filter. In our implementation procedure, this relationship is given by

$$f_p = \frac{2.90}{a}. \qquad (7)$$

Forty-seven values of $a$ were spaced logarithmically to cover a frequency range from 2.9 Hz to about 0.022 Hz. The large scale cut-off was determined by the number of points in the sampled time series. More information about the application of wavelet analysis to the study of turbulence is given in (Farge, 1992).

## 5. CHARACTERIZATION OF ATMOSPHERIC TURBULENCE WITH WAVELETS

Contour plots of the wavelet energy density of the $u$- and $v$- velocity components in figures 1-a and 1-b are shown in figures 6-a and 6-b. The axes are time in seconds and the natural log of the scale, $a$. The plots show that scales corresponding to frequencies below 0.15 Hz contribute significantly but intermittently to the signal. Such contribution is seen in the high peaks at various times. The plots also show the presence of smaller scales indicated by the streaks. These scales correspond to the frequency range between .25 and 1.0 Hz. By examining time records of the velocity components in the atmospheric wind it can be noticed that the fluctuations are intermittent. By intermittency, we mean that the energy is not evenly distributed in time or space, Farge (1992); Following Townsend (1956), we define an intermittency factor as the percentage of time a measuring device sees the variable in its higher amplitude state.

Because turbulence fluctuations contain different time scales, we have opted to examine the intermittency of the whole time record. In order to estimate the percentage of time where these scales are in their higher amplitude state, it is necessary to define a threshold value and time of integration of energy. Here, the threshold is defined as twice the average energy content of that scale. The time of integration of a scale is taken to be equal to the inverse of the peak frequency of the magnitude of the Fourier transform of the wavelet. It must be recognized that the measured intermittency factor is dependent on the choice of threshold. However, varying the threshold value between 1.5 and 2.5 times the average did not cause significant variations in the measured intermittency factor. Once intermittent peaks in the wavelet transform energy were located, the total energy in these peaks were calculated. Figures 7-a and 7-b show the intermittency factor and percentage of energy content in the peaks of wavelet transform energy of the $u$- and $v$-velocity components shown in figures 1-a and 1-b. The results show that all scales are intermittent, i.e. energy is not distributed evenly in time. The measured intermittency factor, for both $u$- and $v$-components, varies around 0.12 for the smaller scales ($\ln a \leq 3.9$) and is slightly higher, up to 0.2, for the larger scales. Another feature is the percent of energy contained in these intermittent peaks. For the larger scales, the amount is 40 to 50%. These results imply that up to 50% of the total energy of these scales appears over less than 20% of the time.

## 6. WAVELET ANALYSIS THE VELOCITY-PRESSURE RELATION

In order to better assess the velocity-pressure relation, the wavelet cross scalogram of the continuous wavelet coefficients, $\mathcal{W}_u\mathcal{W}_p^*$ is used. The cross scalogram gives peaks where fluctuations from two time series fluctuate at the same time and same scale. If fluctuations do not appear at the same time and same scale, the magnitude of the cross-scalogram is very low. Figures 8-a and 8-b show the $u-p$ and $v-p$ cross-scalograms

for the records shown in figures 1-a, 1-b, and 1-c. The large peak in the $u-p$ and $v-p$ cross scalograms appears at times between 450 and 550 seconds By comparison of the $u-p$ and $v-p$ cross scalograms with the pressure time series, figure 1-c, it is noticed that the pressure peaks at $t$ near 480 and 520 have their origin most probably in turbulent events in $u-$ and $v-$ velocity components. These results suggest the $v$- component of the velocity is important to the occurrence of peak pressures and should not be disregarded. Furthermore, the cross scalogram results suggest that there is a clear relation between the time-localized fluctuations of $u$- and $v$-velocity components and the pressure peaks. In particular, peaks in pressure are associated with fluctuations at the *same* scale and time as the velocity fluctuations from which they originate.

## 7. CONCLUSIONS

The above results show that wavelet analysis is better suited than Fourier decomposition for the characterization of atmospheric turbulence events and modeling the velocity-pressure relation. With wavelet analysis, we are able to show that:

Atmospheric turbulence is highly intermittent. Up to 60% of the energy of large and intermediate scales appears over less than 20/time.

The peaks in the energy distribution of the velocity fluctuations are related to low pressure peaks observed in the pressure coefficients.

Simulation of these events, along with Reynolds number, mean flow parameter, geometry and turbulence intensity, in wind tunnel experiments or in numerical analysis will improve the prediction of peak pressure coefficients.

Both $u$- and $v$- turbulence characteristics should be considered in the simulation.

While the wavelet analysis has been applied for the purpose of improving the analysis and simulation of wind loads on low-rise structures, such analysis can be used to characterize the response of bridges and tall buildings to wind forces. Using wavelet analysis, higher-order statistical analysis, perturbation techniques or a combination of them should improve significantly the undestanding of the dynamical behavior of structures subject to wind forces. One example on the modeling and identification of damping and nonlinear parameters of a three-beam structure with the use of the above techniques is given by Hajj et al (1995).

## 8. ACKNOWLEDGEMENTS

The financial support of the National Science Foundation under Grant # CMS-9412905 is greatly acknowledged. The authors would like to thank Drs. T. Reinhold and K. Mehta for providing the data. The authors would like to also thank Mr. C. Lusk for his help in preparing some of the figures.

## 9. REFERENCES

Farge M., "Wavelet transforms and their applications to turbulence," Ann. Rev. Fluid Mech., 24, 1992, 395-457.

M. R. Hajj, I. M. Janajreh, H. W. Tieleman and T. A. Reinhold, "On the frequency domain analysis of the linear and nonlinear relations between incident turbulence and fluctuating pressures on surface-mounted prisms," Journal of Wind Engineering and Industrial Applications, (in press).

M. R. Hajj, R. W. Miksad, and E. J. Powers, "Measurements and analyses of nonlinear wave interactions with higher-order spectral moments," Journal of Fluids Engineering, ASME. Vol. 119, 1997, 3-14.

M. R. Hajj, A. H. Nayfeh, and P. Popovic, "Identification of nonlinear systems parameters using polyspectral measurements and analyses," Proceedings of the 15th ASME Biennial Conference on Mechanical Vibration and Noise, Boston, MA, 17-21 September 1995, 651-661.

Kawai, H., "Pressure fluctuations on square prisms - applications of strip and quasi-steady theories," J. Wind Eng. Ind. Aerodyn., 13, 1983, 197-208.

Levitan, M. L. and Mehta, K. C., "Texas Tech field experiments for wind loads: building and pressure measuring systems," 8th International Conference on wind engineering, London, Ontario, Canada, 1991.

Smith, D. A., and Mehat, K. C., "Stochastic models for stationary and nonstationary wind data," 7th US National Conference on Wind Engineering, Los Angeles, CA, 1993.

Tieleman, H. W., "Universality of velocity spectra," J. Wind Eng. Ind. Aerodyn., 56, 1995, 55-69.

Townsend, A. A., "The structure of turbulent shear flows," Cambridge University Press, 1956.

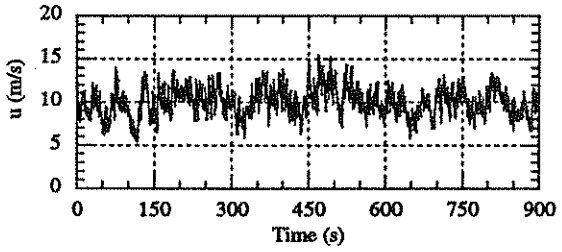


Figure 1-a: Time trace of the u-component of atmospheric wind.

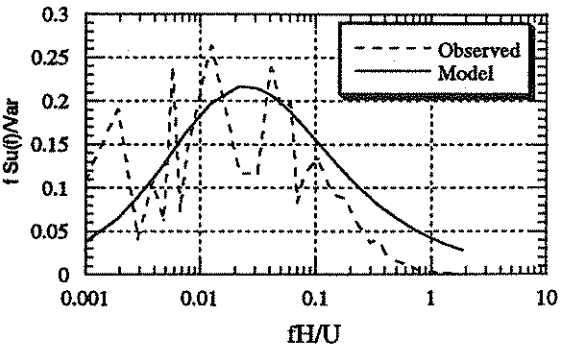


Figure 2-a: Observed and model spectra of the u-component of atmospheric wind

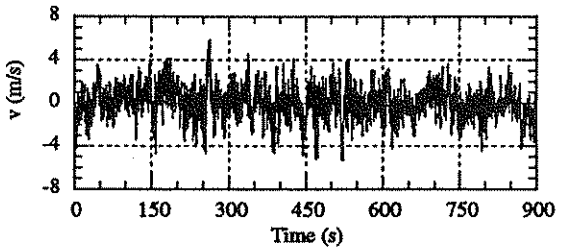


Figure 1-b: Time trace of the v-component of atmospheric wind.

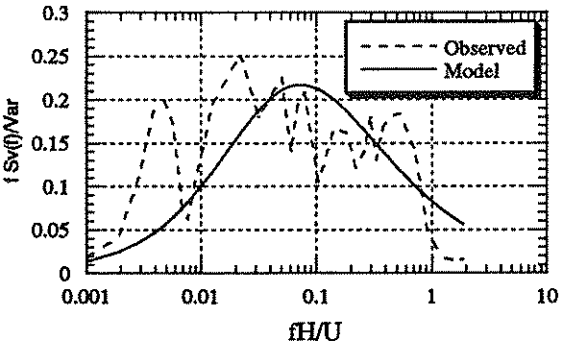


Figure 2-b: Observed and model spectra of the v-component of atmospheric wind

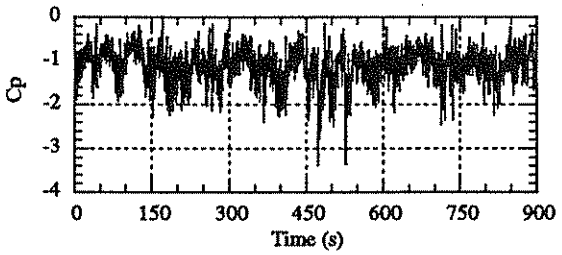


Figure 1-c: Time trace of the corresponding pressure coefficient at y/H = 0.318. (normal incidence)

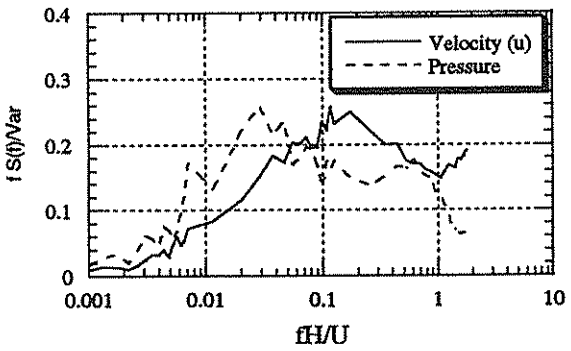


Figure 3: Spectra of the u-component and pressure from the Clemson tunnel.

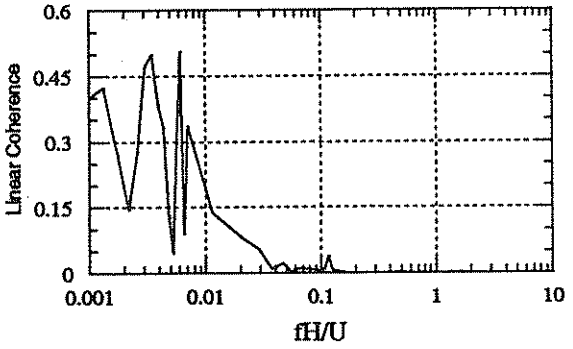


Figure 4: Linear coherence between spectral components of the u-component of the velocity and pressure fluctuations.

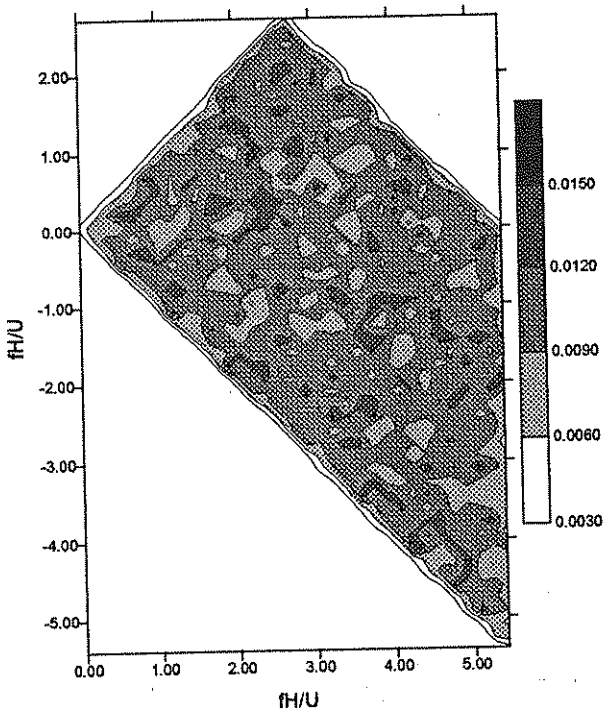


Figure 5: Cross-bicoherence between spectral components of the u- component of the velocity and pressure fluctuations

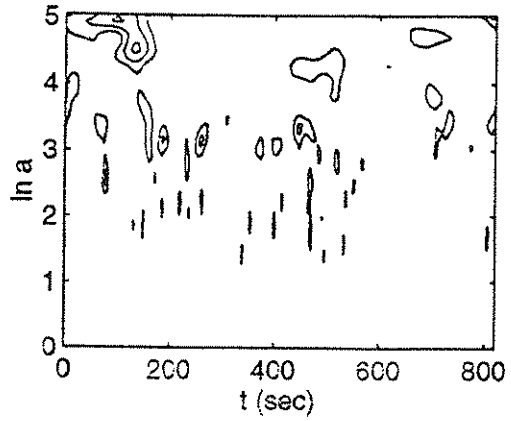


Figure 6-a: Wavelet energy density of the u-component of atmospheric wind (figure 1-a).

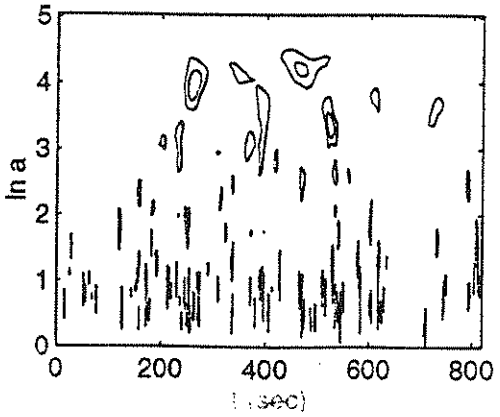


Figure 6-b: Wavelet energy density of the v-component of atmospheric wind (figure 1-b).

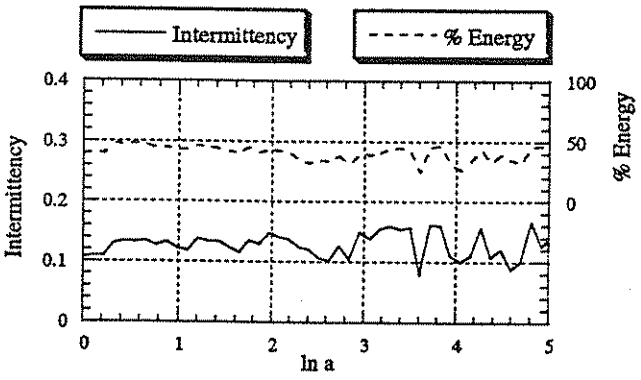


Figure 7-a: Intermittency factor and percent energy content of the u-component of atmospheric wind.

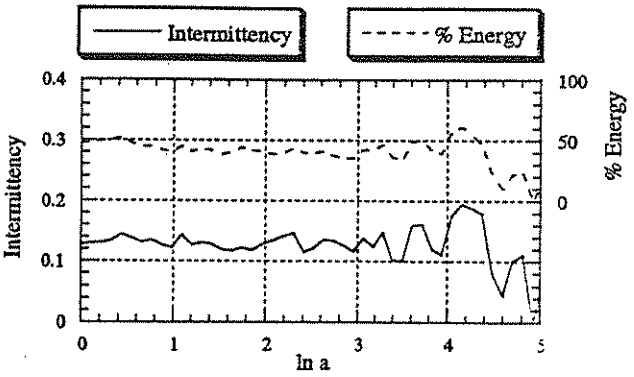


Figure 7-b: Intermittency factor and percent energy content of the v-component of atmospheric wind.

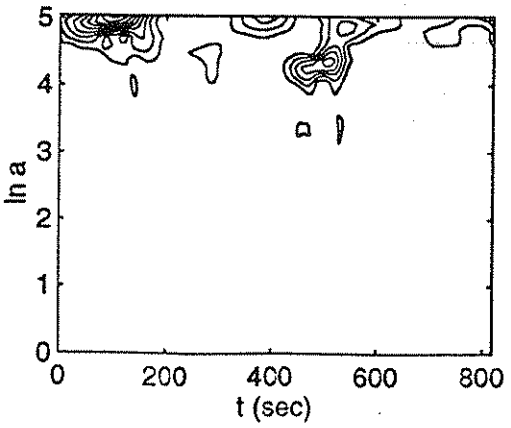


Figure 8-a: Cross scalogram of the wavelet coefficients of the u-component and pressure (figures 1-a and 1-c).

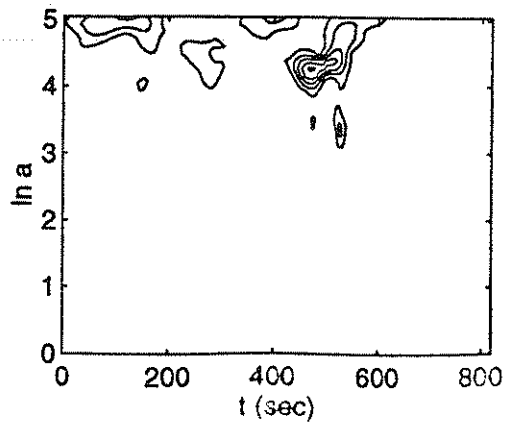


Figure 8-b: Cross scalogram of the wavelet coefficients of the v-component and pressure (figures 1-b and 1-c).